Hindawi Publishing Corporation
ISRN Physical Chemistry
Volume 2014, Article ID 743532, 12 pages
http://dx.doi.org/10.1155/2014/743532

Research Article

Adsorption of Brilliant Green onto Luffa Cylindrical Sponge: Equilibrium, Kinetics, and Thermodynamic Studies

Olaseni Segun Esan,[1] Oladoja Nurudeen Abiola,[1] Olanrewaju Owoyomi,[2] Christopher Olumuyiwa Aboluwoye,[1] and Medinat Olubunmi Osundiya[1]

[1] *Chemistry Department, Adekunle Ajasin University, P.M.B 001, Akungba-Akoko, Nigeria*
[2] *Department of Chemistry, Obafemi Awolowo University, P.M.B 432, Ile Ife, Nigeria*

Correspondence should be addressed to Olaseni Segun Esan; lincolnolaseni@yahoo.com

Received 27 November 2013; Accepted 19 January 2014; Published 4 March 2014

Academic Editors: J. J. Lopez Cascales, L. K. Shrestha, and N. A. Vodolazkaya

The sponge of Luffa cylindrical (LFC), a fibrous material, was employed as adsorbent for the removal of Brilliant Green (BGD) from aqueous effluent via batch studies. The optimum removal of BGD was found at pH 8.2 and the equilibrium was attained within 3 hours. The kinetic data are analyzed using several models including pseudo-first-order, pseudo-second-order, power function, simple elovich, intraparticle diffusion, and liquid film diffusion. The fitting of the different kinetics models to the experimental data, tested by error analysis, using the linear correlation coefficient (r^2) and chi-square analysis (χ^2), showed that the mechanism of adsorption process was better described by pseudo-second-order and power function kinetic models. The equilibrium isotherm data were analyzed using Langmuir, Freundlich, and Temkin models and the sorption process was described by the Langmuir isotherm with maximum monolayer adsorption capacity of 18.2 mg/g at 303 K. The thermodynamic properties ΔG^0, ΔH^0, and ΔS^0 showed that adsorption of BGD onto LFC was spontaneous, endothermic, and feasible within the temperature range of 303–313 K.

1. Introduction

Worldwide, over 7×10^5 tons of dyes and pigments are produced annually [1] and an estimated 90% of this ends up on fabrics [2]. Due to the development of textile, printing, and tanning industries, large amounts of dye water waste are produced [3]. The textile industry alone accounts for two-third of the total dye stuff production and about 10 to 15% of the used dyes come out through the effluent [4]. Wastewater containing dyes is difficult to treat, since the dyes are recalcitrant organic molecules, resistant to aerobic digestion and are stable to light, heat, and oxidizing agents [5]. Efficient color removal from wastewaters is, therefore, of high importance, and so in recent years, it has attracted increased research and technological interest, involving physical and/or chemical methods (i.e., coagulation/flocculation) [6], adsorption [7], oxidation [8], and membrane based separation [9–11].

Amongst all these treatment methods, adsorption is the most appropriate and efficient technique for the removal of nonbiodegradable pollutants (including dyes) from waste water [12, 13]. Although many adsorbents have been reported for removing some common dyes [14–19], such as methyl orange, methylene blue, Congo Red, and Brilliant Green (Figure 1), activated carbon has proven to be the most widely used adsorbent for the removal of dye but this has been restricted due to regeneration problem and high cost [20].

Recently, researchers have focused on the development of cheaper, nonconventional, low-cost adsorbents as an alternative to activated carbon. Some of these include powdered peanut [21], bagasse fly ash [22], palm kernel coat [23], and raw pine cone [24].

Brilliant Green (BGD) which appears as golden crystal is an organic dye that belongs to the family of triphenylmethane [25] and has been used for various purposes, for example, biological stain, dermatological agent, veterinary medicine, and an additive to poultry feed to inhibit propagation of mold, intestinal parasites, and fungus [19]. This dye is known to be toxic to humans and animals when injected. It causes irritation to the gastrointestinal tract and upon prolonged exposure resulted in organ damage [26]. Upon decomposition of

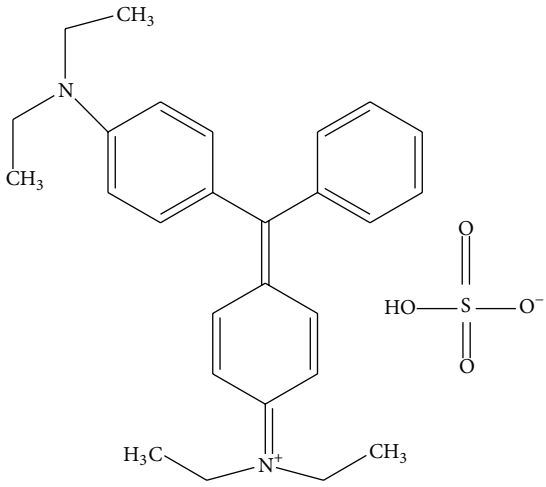

Figure 1: Brilliant Green.

this dye, carbon dioxide, sulphur oxides, and nitrogen oxides are produced [27].

Luffa cylindrical (LFC) belongs to the Cucurbitaceae family [28] and is commonly grown in China, Japan, Nigeria, and countries in central and South America. LFC sponge is composed mainly of cellulose, hemicelluloses, and lignin [29]. On this note, LFC is called lignocelluloses material. Because it has a fibrous vascular system that can allow the removal of water pollutants. Various researchers utilized Luffa cylindrical in different forms to remove dyes from solution. Like Ola [30] used luffa activated carbon, Demir et al. [29] used NaOH treated luffa and Oladoja et al. [17] used untreated luffa to remove dyes from solution.

Owing to the toxicity of BGD dye, it is essential to remove BGD from waste water. Early, Bhattacharyya and Sarma [31] have used finely ground neem leaf, Kismir and Aroguz [27] used saklikert mud, Mittal et al. [26] used bottom ash and deoiled soya, and Mane et al. [32] used rice husk ash as low-cost adsorbent for removing BGD from aqueous media. In the present study, Luffa cylindrical powder shall be studied as adsorbent for BGD removal.

However, this study is detailed to investigate the possibility of utilizing LFC for the removal of BGD from aqueous solution by performing batch studies. The effect of different experimental conditions, such as contact time, initial pH, initial dye concentration, and temperature were investigated, and the adsorption mechanism was examined using kinetic and thermodynamic studies.

2. Materials and Methods

2.1. Sorbent Preparation. LFC was obtained locally from Akungba-Akoko, the University town, Nigeria. The LFC was dehusked and the intervening tissue was removed [17] while the LFC fibers were washed with water to remove all the water soluble contaminant, until the washing became clear, and dried in the oven at 70°C for 6 h [29]. The dried LFC fibers were ground with Laboratory blender and screened through a set of sieves to obtained particles of size 100 μm.

2.2. Dye Solution and Reagents. BGD [Sulfate of N,N-diethylaniline] is a cationic dye classified as C.I. basic green 1; (C.I. 42040; FW: 462.65 and 625 nm λ_{max}) was obtained from Fine Chemical, Mumbai, India and used without further purification. Stock solution, (500 mg/L), was prepared and working solutions were prepared from the stock by serial dilution. The pH of the solution was adjusted when required by adding drops of HCl (1.0 M or 0.1 M) or NaOH (1.0 M or 0.1 M) solutions. Changes were monitored with a pH meter (Jenway, model 710, USA).

2.3. Dye Quantification. The BGD concentration in aqueous solution was quantified by the determination of the optical density at the characteristic wavelength using a double beam UV/visible spectrophotometer. A standard solution of the dye was taken and the optical density was determined at different wavelength to obtain a plot of optical density versus wavelength. The wavelength corresponding to the maximum optical density (λ_{max} = 625 nm), as determined from this plot, was noted and the wavelength was used for the preparation of the calibration curve used in the present studies.

2.4. Characterization of Adsorbent (LFC)

2.4.1. Point of Zero Charge (PZC) Determination and FTIR Study. The pH_{ZPC} shows considerable usage for the determination of surface electrical neutrality at a definite pH value. The determination of zero point charge (pH_{ZPC}) was done via the solid addition method [33]. Possible involvement of functional groups from LFC during the removal of BGD from aqueous solution was elucidated using the Fourier transform infrared (FTIR) analysis. FTIR spectra were obtained on a PerkinElmer FTIR-600 spectrometer. The analysis conditions used were 16 scans at a resolution of 4 cm^{-1} measured between 400 and 4000 cm^{-1}.

2.5. Adsorption Experiments. Batch adsorption experiment studies were conducted by agitating 0.1 g of adsorbent with 50.0 mL of BGD solution of the desired initial dye concentration of 20–200 mg/L in a 250 mL stoppered conical flask. The mixture was agitated in a temperature controlled orbital shaker at a constant speed of 160 rpm at required temperature. Samples were withdrawn at regular interval and centrifuged and the residual BGD concentration was calculated from the calibration curve [34]. The kinetics of adsorption was conducted by analyzing adsorptive uptake of the dye from the aqueous solution at different time intervals (2, 5, 10, 30, 60, 90, 120, and 180 min). For studying the effect of solution pH on dye adsorption, experiment was conducted at different pH varying from 4.2 to 9.3 for initial dye concentration of 200 mg/L. To observe the effect of temperature on dye adsorption, sorption characteristic was investigated by determining the adsorption isotherms at 303, 313, 323, and 333 k. The amount of sorbate sorbed per unit mass of the LFC

(q_t in mg/g) and percentage dye removal efficiency, R, was calculated using the mass balance procedure as follows:

$$q_t = \frac{(C_0 - C_t)V}{M},$$
$$R = \left(\frac{C_0 - C_t}{C_0}\right) \cdot 100, \quad (1)$$

where C_0 is the initial dye concentration (mg/L), C_t is the concentration of dye at any time t, V is the volume of solution in (L), and M is the mass of BGD (g).

2.6. Error Analysis. In the present study, each of the isotherm models was tested using the linear coefficient of determination, r^2, and the chi-square statistical method, χ^2. The coefficient of determination, r^2, represents the percentage of variability in the dependents variable that has been explained by regression line. The value of the coefficient of determination may vary from zero to one. The linear coefficient of determination, r^2, found from evaluation of data by linear model, was calculated with the aid of the following equation:

$$r^2 = \frac{S_{xy}^2}{S_{xx}S_{yy}}, \quad (2)$$

where S_{xx} is the sum of squares of x, S_{yy} is the sum of square of y, and S_{xy} is the sum of squares of x and y.

In order to evaluate the best of the isotherm models that fit the experimental data, the sorption process was also examined using nonlinear chi-square statistical test. The chi-square statistic test is basically the sum of the squares of the differences between the experimental data and data obtained by calculating from models, with each squared difference divided by the corresponding data obtained by calculating from models. The equivalent mathematical statement is

$$\chi^2 = \frac{\sum \left(q_{e,\exp} - q_e\right)^2}{q_e}. \quad (3)$$

If data from model are similar to the experimental data, then χ^2 will be a small number, and if they are different, χ^2 will be a bigger number.

3. Result and Discussion

3.1. Results of Point of Zero Charge (pH_{PZC}) Determination and FTIR Analysis. The point of intersection of ΔpH versus pH_0 showed that the pH_{ZPC} of LFC occurred at pH 5.2 as shown in Figure 2. This showed that at pH less than 5.2 the surface of LFC is predominated by positive charges while at pH greater than 5.2, the surface is predominated by negative charges.

It was clear from Figures 3 to 4 that FTIR spectra of the LFC before and after adsorption of BGD displayed a number of absorption peaks, reflecting the complex nature of the material examined. They are carbonyl and hydroxyl groups, on the surface of LFC from FTIR analysis [35]. The broad absorption peaks around 3423 cm^{-1} were indicative

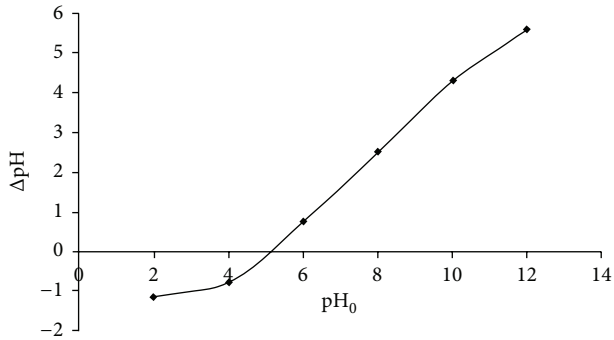

Figure 2: Results of the determination of the pH_{ZPC}.

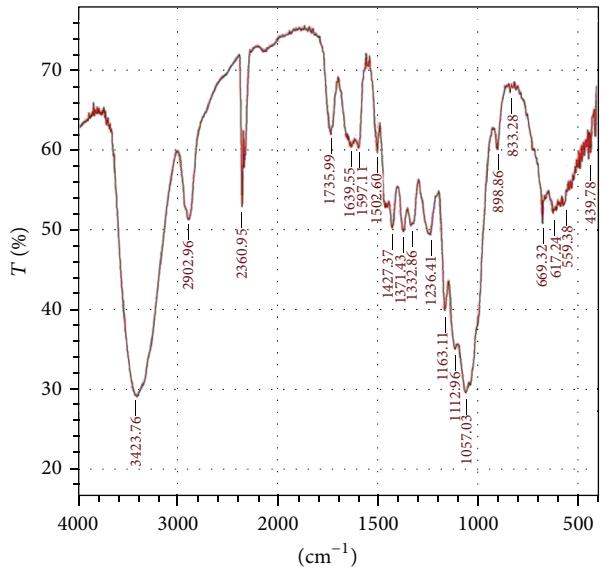

Figure 3: FT-IR of Luffa cylindrical (LFC) before adsorption of BGD.

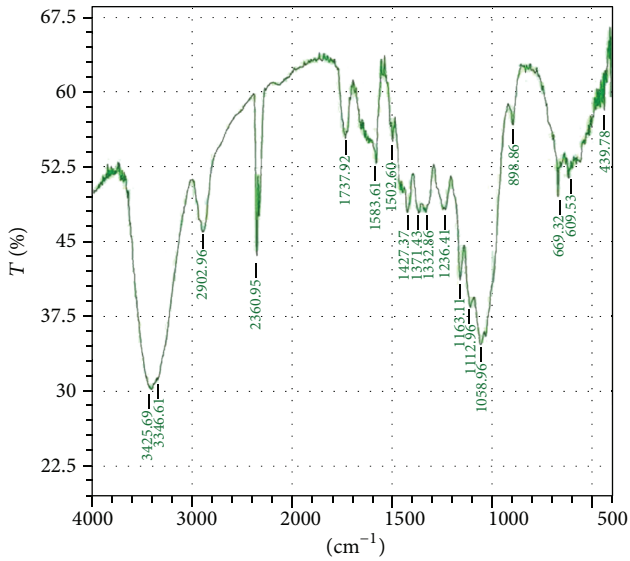

Figure 4: FT-IR of Luffa cylindrical (LFC) after adsorption of BGD.

of existence of bonded hydroxyl groups on the surface of LFC. The peaks at 2902 and 2360 cm^{-1} were assigned to the stretching vibration and bending vibration of C–H bond in methylene group, respectively. The broad band at 1735 cm^{-1} was assigned to the carbonyl and carbonyl moieties (C=O). The peaks associated with the stretching vibration in aromatic rings were verified at 1597 and 1425 cm^{-1}. The peak at 1236 cm^{-1} was assigned to the bending vibration of carboxylic groups while deformation related to C–O bond was observed at 1057 cm^{-1} which also confirmed the lignin structure of the LFC. All of these surface functional groups of the LFC can interact with the BGD molecules. Thus, the adsorption of BGD on LFC may be attributed to (i) chemical interaction between surface functional groups and BGD molecules (ii) electrostatic interaction between the BGD molecules and electron-rich sites on the LFC surface, and (iii) week physical forces, mainly hydrogen bonding and van der Waals interactions between the BGD molecules and the LFC. Therefore, the adsorption of BGD onto LFC surface may emanate from the interaction between the carboxyl group of LFC and the electronegative groups in BGD, hydrogen bonding between the hydroxyl group of LFC and the nitrogen of the BGD molecules, and hydrogen bonding between the hydroxyl group of the LFC and the aromatic ring in the BGD molecule. This has confirmed that adsorption of BGD onto LFC follows a complicated pattern which involved both physical and chemical.

3.2. Effect of pH on the Adsorption Capacity. It is a known fact that solution pH is an important variable in sorption studies. The pH of the solution affects surface charge of the adsorbent, the degree of ionization of adsorbate molecule, and extent of dissociation of functional groups on the active sites of the adsorbent [19]. The dye uptake variations at different pH value and initial concentrations of 200 mg/L are shown in Figure 5. The adsorption rate changed at the beginning, from 11.5% at pH 2.0 to 89.9% at pH 6.97. With a further increase of pH from 6.97 to 10.0, the adsorption rate decreased. Consequently, pH 6.97 was selected as the operating pH for subsequent studies.

The possible explanations are as follows. (i) LFC has an estimated point of zero charge of pH 5.2, above which LFC surface is predominantly negatively charge, leading to a favorable electrostatic interaction between the cationic BGD molecule and the LFC, hence there is a linear increase in BGD uptake as shown in Figure 5. (ii) In an acidic and at lesser alkaline medium, the Cl^- and OH^- from HCl and NaOH destroy the conjugated bond present in the aromatic rings of the dye molecule upon which the BGD structure changed and result in the formation of colorless compound [36], leading to increase in the uptake of BGD molecule from solution as shown in Figure 5. (iii) The presence of carboxyl groups on the surface of LFC, as confirmed by Figures 3 and 4 also, enhances sorption of BGD with increase in pH from 2 to 8 and later decrease at pH 10. This is because the pk_a value of carboxyl groups lies within the range of 3.8–5.0 [37]. Below pH 5.0, the carboxyl group on the surface of LFC gets protonated (H^+) making the number of positive charge sites

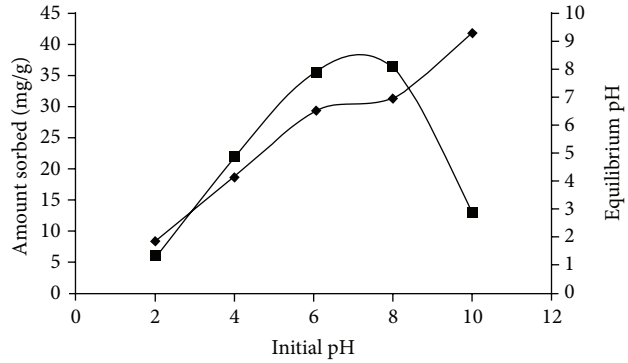

Figure 5: Effects of initial solution pH on the sorption of BGD onto LFC.

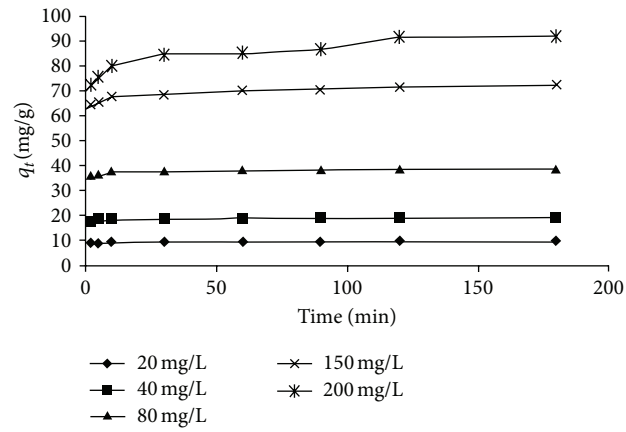

Figure 6: Effect of contact time on the removal of BDG onto LFC.

increase and the number of negative charge decrease resulting in electrostatic repulsion, hence decrease in BGD uptake by LFC. With an increase in pH of the solution, these functional groups became deprotonated (COO^-), which resulted in an increase in the negative charge density on the LFC surface and facilitated the binding of BGD dyes [38]. Hence, the BGD ions binding to the adsorbent could be assumed to involve electrostatic interaction between cationic dyes and negatively charged COO^- groups.

The results of the equilibrium pH (i.e, pH_f) at different initial solution pH (2–10) ranged between 2.39 and 9.3 for BGD/Luffa system as shown in Figure 5. The pH_f values were higher than pH_0 values for $pH_0 < 8.0$ and this could be attributed to change in the structure of dye molecule.

3.3. Effect of Initial Dye Concentration and Adsorption Kinetics. The rates of sorption of BGD by LFC at different initial BGD concentrations are shown in Figure 6. Uptake of BGD was rapid and equilibrium was attained within 180 min. It was found that the amount BGD sorbed increased from 9.2 to 92.9 mg/g with increasing initial concentration from 20–200 mg/L. The adsorption was initially rapid and then slowed down over time. This observation was ascribed to a large number of available binding sites for adsorption during the initial stage, and then the remaining sites were difficult

Table 1: Kinetic parameters of sorption of BGD on LFC.

Initial conc.	Pseudo-first-order			Pseudo-second-order				Power function			Simple Elovich	
mg/L	q_{e_1}	$k_1 \times 10^{-2}$	r^2	q_{e_2}	k_2	h_0	r^2	a	b	r^2	A	B
20	1.54	0.2303	0.820	9.621	0.132	12.20	0.999	8.79	0.016	0.920	8.80	0.799
40	1.86	0.2303	0.794	19.230	0.097	35.87	1.000	17.78	0.014	0.911	17.78	1.462
80	3.07	0.4606	0.747	40.000	0.057	91.20	1.000	35.73	0.015	0.916	35.70	3.001
150	7.50	1.1515	0.966	76.920	0.011	65.08	0.999	63.39	0.025	0.977	63.26	9.046
200	17.82	1.1612	0.916	100.000	0.004	40.00	0.999	70.15	0.051	0.967	69.51	22.48

$k_1 = \text{min}^{-1}$, $q_{e_1} = \text{mg/g}$, $q_{e_2} = \text{mg/g}$, $k_2 = \text{g/mg/min}$, $B = \text{g/mg}$, $A = \text{mg/g min}$.

to occupy due to repulsive forces between the dye molecules on the LFC and the bulk phase [39]. The results showed that the time taken to attain equilibrium was independent of the initial dye concentration. Similar profile has been reported in the literature for the effect of time and initial concentration for the removal of BGD by adsorbents like kaolin [19], bottom ash and deoiled soya [26], neem leaf powder [31], and modified peat-resin [40].

In order to explore the kinetics involved in dye sorption, the experimental data were fitted into four kinetic models including the pseudo-first-order equation [41], pseudo-second-order equation [42], power function [43], and simple Elovich [44].

The linear form of the pseudo-first-order kinetic is expressed as follows:

$$\ln\left(q_e - q_t\right) = \ln q_e - k_i t, \tag{4}$$

where q_e and q_t are BGD adsorbed at equilibrium and time t, respectively (mg/g), and k_1 is the rate constant for the pseudo-first-order model (min^{-1}). The pseudo-first-order constant k_1 and the correlation coefficient, r^2, deduced from the kinetic data are presented in Table 1. The r^2 value was poor and ranged between 0.747 and 0.966. A significant chi χ^2 values were also obtained indicating the inapplicability of this model to the sorption process.

The pseudo-second-order kinetic model is represented by the following linear equation:

$$\frac{t}{q_t} = \frac{1}{k_2 q_e^2} + \frac{1}{q_e t}, \tag{5}$$

where k_2 is the rate constant for the pseudo-second-order model (g(mg min)^{-1}), where q_e, q_t, and t have the same meaning as explained above.

The initial sorption rate can be obtained from the pseudo-second-order linear plots as q_t/t approaches zero:

$$h_0 = k_2 q_e^2, \tag{6}$$

where h_0 = initial sorption rate.

Equation (3) can be rearranged to obtain [45] as follows:

$$q_t = \frac{1}{1/h_0 + t/q_e}. \tag{7}$$

The r^2 values for the pseudo-second-order kinetic model were close to 1.0 for all cases. Comparing r^2 and chi χ^2 value for pseudo-first- and second-kinetic model (Table 1), it is obvious that for the entire adsorption period, the pseudo-second-order model fits the experimental data better than the pseudo-first-order model. It thus shows that the system under study was more appropriately described by the pseudo-second-order model. This indicates that the adsorption mechanism for BGD is chemisorptions, involving covalent forces through sharing or exchange of electrons between sorbent and sorbate [46].

The value of h_0, q_e, and k_2 along with r^2 for the pseudo-second-order models are shown in Table 1. The value of q_e increased with increase in the initial BGD concentration while h_0 increase from 12.20 to 91.20 and later decreased drastically to 40.00 with the increases in initial concentration of BGD. According to Ho and Mckay [47] if the dye uptake is chemically rate controlled, the pseudo-second-rate constant will be independent of particle diameter and flow rate will depend on concentration of the ions in solution.

Logarithm plots of pseudo-second-order constants, k_2, and h_0, versus C_0 of BGD concentration were made, and the plots were found to be straight line whose linear regression values r^2, in terms of C_0, were given as 0.992 and 0.946, respectively [45].

Mathematical expressions were therefore drawn relating the two pseudo-second-order constants and initial concentration as follows:

$$\begin{aligned} k_2 &= -0.008 C_0^{-0.656}, \\ h_0 &= -4.228 C_0^{8.408}. \end{aligned} \tag{8}$$

Linear plots of q_{e_2}, k_2, and h_0 against initial concentration (C_0) were regressed to obtain these values in terms of C_0 with high concentration coefficient. Each of these parameters can be expressed as a function of C_0 for BGD as reported by Ho and McKay [47];

$$q_e = \frac{C_0}{E_q C_0 + F_q}, \tag{9}$$

$$k_2 = \frac{C_0}{E_k C_0 + F_k}, \tag{10}$$

$$h_0 = \frac{C_0}{E_h C_0 + F_h}, \tag{11}$$

where E_q, F_q, E_k, F_k, E_{h_0}, and F_{h_0} are constants related to the respective equations. The values for these constants are

Table 2: Empirical parameters for predicted q_e, k, and h_0 from C_0 for BGD dye.

E_q (g/mg)	F_q (g min/L)	r^2	E_k (mg min/g)	F_k (mg^2 min/gL)	r^2	E_{h_0} (g min/mg)	F_{h_0} (g min/L)	r^2
0.507	0.594	0.946	16.0×10^{-4}	0.128	0.921	1.326	15.46	0.998

Table 3: Error analysis for the kinetic data of the sorption of BGD on LFC.

Initial conc.	Pseudo-first $q_e = q_e(1 - e^{-k_1 t})$		Pseudo-second $q_e = tk_2q_e^2/(1 + tk_2q_e)$		Power function $q_e = at^b$		Simple Elovich $q_e = A + B\ln t$	
(mg/L)	χ^2	r^2	χ^2	r^2	χ^2	r^2	χ^2	r^2
20	12.376	0.997	1.83×10^{-4}	0.999	5.28×10^{-4}	1.000	1.150	1.000
40	24.698	0.997	1.89×10^{-4}	1.000	3.55×10^{-4}	1.000	1.490	1.000
80	12.985	0.987	2.39×10^{-5}	1.000	4.51×10^{-4}	1.000	3.19	1.000
150	1.311	0.940	3.50×10^{-3}	0.999	1.26×10^{-3}	1.000	12.93	1.000
200	0.294	0.910	2.06×10^{-2}	0.999	3.48×10^{-3}	1.000	47.71	1.000

listed in Table 2. Hence the generalized predictive model for BGD sorbed at any contact time and initial concentration within the given range with relationship of q_e, C_0, and t can be represented as follows by substituting the various values in (10).

For BGD-LFC system [47]:

$$q_t = \frac{t}{1/\left(1.326C_0 + 15.46\right) + 1/\left(0.507C_0 + 0.594\right)t}. \quad (12)$$

Equation (12) represents the generalized predictive model for BGD sorbed at any time and the initial BGD concentration within the given range.

To further establish the appropriate kinetic for BGD uptake, the experimental data was fitted again to power function and simple Elovich models.

The power function model is a modified form of the Freundlich equation and may be expressed as:

$$\log q = \log a + b \log t \quad (13)$$

while the simple Elovich [45] is expressed as:

$$q = A + 2.303B \log t. \quad (14)$$

The results obtained for the fitting of the kinetic models to explained data are presented in Table 1 and the error functions are presented in Table 3. For the pseudo-first-order kinetic and simple Elovich models, the predicted q_e values were at variance coincident with the experimental q_e values. The predicted q_e values derived from pseudo-second-order and power function model agreed with the experimental q_e data. The values χ^2 of the error function were negligible for pseudo-second-order and power function model. This result indicates that the pseudo-second-order and power function model provided a high degree of correlation with the experimental data for the sorption of BGD by LFC.

3.4. Intra-Particle Diffusion Model. Intraparticle diffusion model based on the theory proposed by Weber and Morris which has been widely applied for sorption studies was applied to investigate the mechanism of the adsorption of BGD onto LFC. The intraparticle diffusion model is typically given as follows [48]:

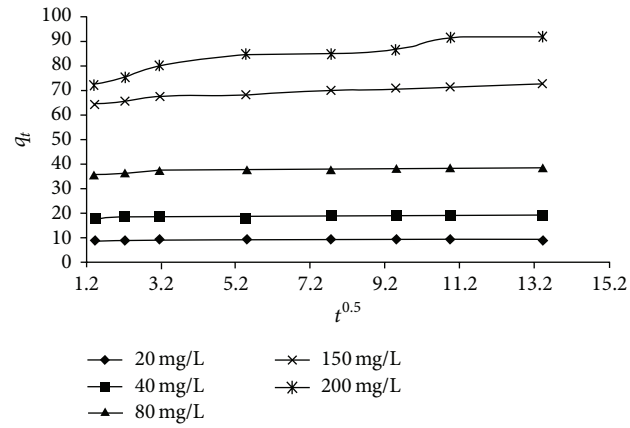

Figure 7: Plot of q_t versus $t^{0.5}$ for the adsorption of BGD onto LFC.

$$q_t = k_{\text{id}} t^{0.5} + Z, \quad (15)$$

where Z (mg g^{-1}) is the intercept and k_{id} (mg g^{-1} min$^{0.5}$) is the intraparticle diffusion rate constant. Value of k_{id} was obtained from the slope of the linear plot of q_t versus $t^{0.5}$ (Figure 7). Value of Z as shown in Table 3 gives an idea about the thickness of the boundary layer [49]. The deviation from this theory signifies the difference between the rate of mass transfer in the initial and final stage of adsorption [50].

However, if the data exhibit multilinear plots, then two or more steps influence the sorption process. The first, sharper portion is attributed to the transport of the solute from bulk solution liquid film to the adsorbent exterior surface. The second linear portion is based on the diffusion across the liquid film surrounding the sorbent particle. The third portion is due to particle diffusion in the liquid contained in the pore and in the sorbate along the pore wall.

Figure 7 shows a representative q_t versus $t^{0.5}$ plot for BGD adsorption onto LFC for C_0 = 20, 40, 80, 150, and 200 mg/L at 30°C. Observation from the figure shows that the plots were not linear over the whole time range; an indication that more

Table 4: Macro- and micropores diffusion parameters for the sorption of BGD by LFC at different initial BG concentration (mg/L).

Initial conc. (mg/L)	k_{id_1}	Intercept	r^2	k_{id_2}	Intercept	r^2
20	0.225	8.54	0.900	0.043	9.04	0.873
40	0.478	17.17	0.901	0.074	18.26	0.932
80	0.953	34.45	0.909	0.115	37.07	0.913
150	1.918	61.68	0.992	0.498	65.97	0.948
200	4.375	66.21	0.990	1.061	78.07	0.835

Table 5: Liquid film diffusion parameters for the sorption of BGD by LFC at different initial BGD concentration (mg/L).

Initial conc. (mg/L)	First 30 mins			Overall		
	k_{id_1}	Intercept	r^2	k_{id_2}	Intercept	r^2
20	0.008	1.85	0.650	0.002	1.93	0.820
40	0.011	2.28	0.465	0.004	2.38	0.794
80	0.017	2.39	0.581	0.005	2.57	0.747
150	0.017	2.19	0.718	0.011	2.28	0.966
200	0.031	1.54	0.943	0.016	1.65	0.916

than one process controlled the sorption process which are: surface sorption and intraparticle diffusion. For C_0 = 80, 150, and 200 mg/L, there are two linear portions, the first straight portion depicting mesopore diffusion and the second represent micropore diffusion [51]. For C_0 = 20 and 40 mg/L, there is only one linear portion depicting combined mesopore diffusion.

There is every possibility that the intraparticle diffusion of BGD into pores is the rate controlling step in the adsorption process. The amount of adsorbate and the driving force for BGD adsorption is less for C_0 = 20 and 40 mg/L as compared to that of C_0 = 80, 150, and 200 mg/L; hence, BGD adsorbed in mesopore only, and adsorption into mesopore is the rate-limiting step. For C_0 = 80, 150, and 200 mg/L, the driving force increases and overcomes the resistance for getting adsorbed into micropores; therefore, adsorption into micropores is the rate-limiting step for higher C_0. An observation from Table 4 shows that K_{id_1} and K_{id_2} are higher for higher C_0, which indicate enhanced diffusion of BGD through meso- and micropores at higher C_0. This is a contribution from higher driving force at higher C_0 [51]. Similar results have been reported for adsorption of BGD on saw dust [52], kaolin [19], and rice husk ash [32].

3.5. Liquid Film Diffusion Model. During sorption, the migration of dye molecules from bulk solution through liquid film to the exterior surface of adsorption may play an important role in determining the rate of the adsorption process. To predict the potential rate-controlling step, the adsorption dynamics of BGD onto LFC was investigated utilizing liquid film diffusion model (16) [53]:

$$\ln(1 - F) = -k_{fd}t, \tag{16}$$

where k_{fd} (min^{-1}) is the liquid film diffusion rate constants and $F = q_t/q_e$. The plot of $-\ln(l - F)$ versus t, for the liquid film diffusion, was tested over all concentration of study. The first 30 mins of sorption process yielded linear plot (r^2 = 0.465–0.943) while the overall yielded (r^2 = 0.747–0.966). The rate constant for liquid film diffusion, k_{fd}, is in the range 8.0×10^{-3} to 1.7×10^{-2} for the first 30 min and 2.0×10^{-3} to 1.6×10^{-2} for overall (Table 5). The inability of the plot to pass through the origin (i.e., zero intercept) shows that the prediction of this model will have only limited applicability in the adsorption of BGD by LFC.

3.6. Adsorption Equilibrium Isotherm Study. The distribution of BGD between the liquid phase and the solid adsorbent phase is a measure of the position of equilibrium in the adsorption process and can be expressed by different equilibrium isotherm models. In this study, the Langmuir, Freundlich, and Temkin isotherms models were used to describe the adsorption process and the isotherm parameters obtained using these models are presented in Table 6.

The linear form of Langmuir's isotherm model is represented by the following equation:

$$\frac{1}{q_e} = \frac{1}{Q_0} + \frac{1}{bQ_0C_e}. \tag{17}$$

The values of monolayer sorption capacities, Q_0 (mg/g), obtained from Langmuir plot of sorption decreased with increasing temperature. The magnitude of Langmuir constant, b, which is the sorption equilibrium constant (dm^3/mg), decreases as shown in Table 6. The decrease of b as temperature increases confirms the exothermic nature of the adsorption [54]. The essential characteristics of the Langmuir isotherm, used to predict the adsorption efficiency, was expressed in terms of a dimensionless equilibrium parameter R_L, defined by the following equation [55]:

$$R_L = \frac{1}{1 + bC_0}, \tag{18}$$

where C_0 (mg/L) is the highest initial concentration of the adsorbate. The value of R_L indicates if the Langmuir isotherm is unfavorable ($R_L > 1$), linear ($R_L = 1$), favorable

Table 6: Adsorption isotherm constants for BGD on LFC.

Temperature (°C)	Langmuir				Freundlich			Temkin		
	Q_0	b	R^2	$R_L \times 10^{-3}$	K_f	$1/n$	R^2	B_I	A	R^2
30	18.52	17.99	0.991	2.7	17.83	0.722	0.958	27.75	2.150	0.984
40	8.85	28.21	0.963	1.7	2.42	1.212	0.972	28.39	1.014	0.931
50	5.68	35.16	0.961	1.4	1.01	0.176	0.964	35.04	1.410	0.944
60	8.50	5.16	0.998	9.4	7.01	0.952	0.928	58.06	1.070	0.987

Table 7: Error analysis for isotherm models for the sorption of BGD on LFC.

Initial conc. (mg/L)	Langmuir; $q_e = Q_L bc_e/(1 + bc_e)$	Freundlich; $q_e = k_f c_f^{1/n}$	Tempkin; $q_e = (RT/b)\ln(K_T c_e)$
	χ^2	χ^2	χ^2
20	0.2664	0.3782	0.4525
40	0.0009	0.1016	0.2386
80	0.0008	1.0420	2.4264
150	0.1251	2.2042	16.5165
200	1.4370	4.1396	126.0713

($0 < R_L < 1$), or irreversible ($R_L = 0$). The values of R_L at C_0 = 200 mg/L in the present study were found to be 2.7×10^{-3} at 303 K, 1.7×10^{-3} at 313 K, 1.4×10^{-3} at 323 K, and 9.4×10^{-3} at 333 K indicating that the adsorption of BGD on LFC is favorable.

The experimental data obtained was also tested with Freundlich isotherm. Freundlich isotherm assumes heterogeneity of adsorption surfaces. The equation is commonly expressed as follows [56]:

$$\log q_e = \log K_f + \frac{1}{n} \log C_e. \tag{19}$$

The values of the Freundlich constant, K_f and n, related to adsorption capacity and sorption intensity, respectively, obtained from the plot of $\log q_e$ versus $\log C_e$ are presented in Table 6. K_f is the Freundlich affinity coefficient, and $1/n$ is the Freundlich linearity index. It can be found that the values of K_f and n decrease, indicating that adsorption is favorable at lower temperature predicting endothermic nature of the adsorption process. Experimental data was also fitted to Temkin isotherm.

The Temkin isotherm assumes that a decrease in the adsorption heat is linear and that the adsorption is characterized by a uniform distribution of binding energies. The Temkin linear form of isotherm is given by equation [57, 58]:

$$q_e = B_I \ln A + B_I \ln C_e. \tag{20}$$

$B_I = RT/b$, T is the absolute temperature (K), and R is the universal gas constant (8.314 J/molK), A is the equilibrium binding constant (L/mg), and B_I is related to the heat of adsorption. The Temkin constants were listed in Table 6. In order to assess the different isotherms and their ability to correlate the experimental results, the theoretical plots for each isotherm have been shown along with the experimental data for the sorption of BGD onto LFC (Figure 7). The r^2 and χ^2 values were shown in Table 7 and the different isotherms correlated with the experimental depicted in Figure 8 confirmed that the sorption of BGD onto LFC was best described by Langmuir isotherm model. The applicability of the Langmuir isotherm assumes that the entire adsorption sites are equivalent and there is no interaction between adsorbed species.

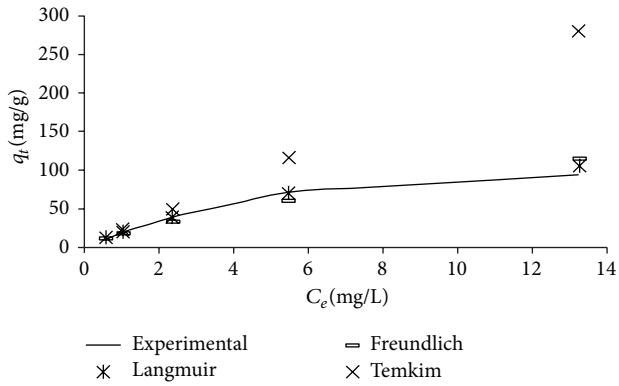

Figure 8: Comparison of experimental data with the theoretical data for equilibrium isotherm studies for the adsorption of BGD onto LFC.

3.7. Estimation of Thermodynamic Parameter. To characterize the thermodynamic parameter of adsorption study means to determine Gibb's free energy, (ΔG^0, KJ/mol), enthalpy change (ΔH^0, KJ/mol), and entropy (ΔS^0, KJ/mol/K) at a given reference temperature and to obtain ΔC_p so as to be able to predict the change of the above three parameters with temperature.

The Gibb's free energy change, ΔG, of an association reaction is temperature dependent and best described by

$$\Delta G^0 = \Delta H^0_{(\mathrm{TR})} + \int_{\mathrm{TR}}^{T} \Delta C_p dT - T\Delta S^0_{(\mathrm{TR})} - T \int_{\mathrm{TR}}^{T} \Delta C_p d \ln T. \tag{21}$$

Table 8: Thermodynamic parameters for adsorption of BGD on LFC.

Temperature (K)	$\ln b$	$-\Delta G^0$ (KJmol^{-1})	ΔH^0 (KJmol^{-1})	ΔS^0 (Jmol^{-1}k^{-1})	ΔC_p (KJk^{-1}mol^{-1})
303	2.89	7.28	108.74	382.91	−8.91
313	3.34	8.69	19.62	90.46	
323	3.56	9.56	−82.27	−225.09	
333	1.64	4.53	−197.03	−578.08	

ΔH^0 and ΔS^0 are the change in enthalpy and entropy, ΔC_p is the heat capacity change. TR is an appropriate reference temperature. In a simple term,

$$\Delta G^0 = \Delta H^0 - T\Delta S^0 \tag{22}$$

which is related to sorption equilibrium constant b at different temperature

$$\Delta G^0 = -RT \ln b. \tag{23}$$

Combining (22) and (23) above, we obtained

$$\ln b = \frac{-\Delta G^0}{RT} = \frac{\Delta S^0}{R} - \frac{\Delta H^0}{R}\frac{1}{T}. \tag{24}$$

T is the absolute temperature (K) and R is universal gas constant (8.314 J/molK). Thus, ΔH^0 can be determined by the slope of the linear Van't Hoff plot, that is, as $\ln K$ versus $(1/T)$, (Figure 9) using equation:

$$\Delta H^0 = \left[R\frac{d\ln K}{d\,(1/T)}\right]. \tag{25}$$

This method is an indirect method but an accurate method to calculate thermodynamics parameters at solid/solution interfaces. Enthalpies of adsorption are assumed to be invariable in relation to temperature. However, difficulties arise from this assumption. Taking into account the curvatures of Van't Hoff plots suggested in Figure 9, a second-order polynomial regression analysis of the Van't Hoff plots was used. The general equation of this type of analysis is $\ln b = A + B\ln(T) + C/T$ where A, B, and C are the regression coefficients. The $-\Delta H^0/R$ values were found from individual regressive function.

The polynomial regression produced better fits (r^2 value from 0.990 to 0.999) in relation to the traditional Van't Hoff plot linear regression (less than 0.900). The curvatures indicate temperature dependence of ΔH^0. Heat capacity, (ΔC_p), which is influenced by the number of accessible energy state, was determined over the range temperature of studies. As an important parameter, it controls the magnitude of ΔH^0 and ΔS^0 [59].

Considering temperature dependence of ΔH^0, an equation can be written to represent nonzero temperature independent ΔC_p:

$$\ln\frac{b_{d_1}}{b_{d_2}} = \frac{\Delta H_i - T_i\Delta C_p}{R}\left(\frac{1}{T_1} - \frac{1}{T_2}\right) + \frac{\Delta C_p}{R}\ln\frac{T_2}{T_1}. \tag{26}$$

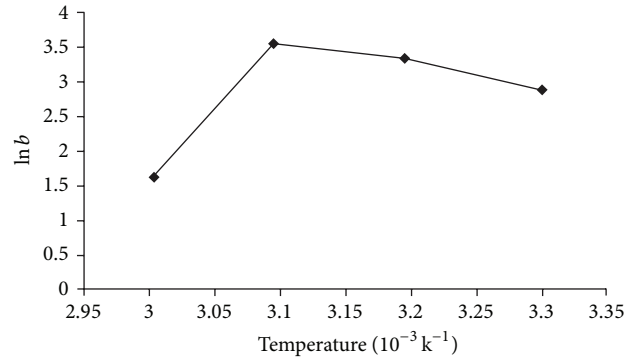

Figure 9: Van't Hoff plot of BGD dye adsorption by LFC.

The ΔC_p value was calculated in a simple manner, as

$$\Delta C_p = \frac{d\left(\Delta H^0\right)}{dT} = \frac{Td\left(\Delta S^0\right)}{dT} = \frac{\Delta H^0_{T_2} - \Delta H^0_{T_1}}{(T_2 - T_1)}. \tag{27}$$

The thermodynamic parameters are shown in Table 8. ΔH^0 is almost all positive and it decreases endothermically within the temperature range of 303 K to 333 K. Explanation for the ΔH^0 obtained within the temperature range of study is based on the fact that BGD and LFC surfaces are both solvated in water. In order for BGD to be adsorbed, they have to lose part of their hydration shell. The dehydration processes of the BGD and LFC surfaces require energy. In general the dehydration processes of the BGD and LFC supersede the exothermicity of the adsorption processes. Overall, it may be assumed that the removal of water from BGD and LFC surfaces is essentially an endothermic processes; this process exceeds that of exothermicity provided by the heat of adsorption as observed in this study. Indication from Table 8 shows that the negative value of ΔC_p couple with favorable positive entropy changes signifies hydrophobic interaction [59]. The negative value of ΔG^0 over all temperature of studies indicates the spontaneous and feasible nature of the adsorption process and that binding of an adsorbate in solution is favored.

The positive ΔS^0 values indicate an increase in disorderliness while negative ΔS^0 value shows decrease in disorderliness. For the interaction of BGD with LFC, ΔS^0 decrease positively; thus, from thermodynamic point of view entropy seems to be the driving force of adsorption [60].

3.8. Mechanism of Adsorption. BGD dye molecule can react with carbonyl and hydroxyl groups available on the surface of LFC. Comparing FTIR before and after adsorption, the peak at 3423 cm^{-1} from –OH remained unchanged but increased

in intensity after adsorption suggesting that –OH group may bind with the immonium ion of the BGD molecule via hydrogen bonding which accounts for the emergence of the new peak at 3346 cm^{-1}. The intensity of the peak at 1737 cm^{-1} assigned to carbonyl group of carboxylic acid decreased while the wavelength shifts to lower wave number after adsorption of BGD, indicating electrostatic interaction between the positively charged nitrogen moiety of the BGD dye molecule and the –COOH group of LFC.

4. Conclusion

LFC, a lignocellulosic material, was used as adsorbent to remove BGD from aqueous solution via batch experimental method. The kinetic studies were performed and the result obtained was fitted to pseudo-first-order, pseudo-second order, power function, and simple Elovich models. Both the pseudo-second-order and power function kinetic models provided excellent data fitting based on the statistical coefficient and chi-square error analysis. The equilibrium data showed that the experimental data correlated reasonably with the Langmuir isotherm model. Nonzero heat capacities term ΔC_p was obtained with the emergence of the plot of $\ln b$ versus $1/T$ and the negative ΔC_p shown in this study indicates absence of thermal dehydration, stable species in solution. Negative value of ΔG^0 suggests spontaneity and feasibility of adsorption process while the positive ΔS^0 predicted that entropy is the driving force adsorption of BGD onto LFC.

Conflict of Interests

The authors declare that there is no conflict of interests regarding the publication of this paper.

References

[1] C. I. Pearce, J. R. Lloyd, and J. T. Guthrie, "The removal of colour from textile wastewater using whole bacterial cells: a review," *Dyes and Pigments*, vol. 58, no. 3, pp. 179–196, 2003.

[2] A. R. Cestari, E. F. S. Vieira, G. S. Vieira, and L. E. Almeida, "The removal of anionic dyes from aqueous solutions in the presence of anionic surfactant using aminopropylsilica-A kinetic study," *Journal of Hazardous Materials*, vol. 138, no. 1, pp. 133–141, 2006.

[3] Q. J. Qian, H. Z. Xiao, Y. X. Xiang, and Z. R. Tie, "Adsorptive removal of cationic dyes from aqueous solutions using graphite oxide," *Journal of Adsorption Science and Technology*, vol. 30, no. 5, pp. 437–447, 2012.

[4] T. K. Sen, S. Afroze, and H. M. Ang, "Equilibrium, kinetics and mechanism of removal of methylene blue from aqueous solution by adsorption onto pine cone biomass of *Pinus radiata*," *Water, Air, and Soil Pollution*, vol. 218, no. 1–4, pp. 499–515, 2011.

[5] T. Akar, A. S. Ozcan, S. Tunali, and A. Ozcan, "Biosorption of a textile dye (Acid Blue 40) by cone biomass of *Thuja orientalis*: estimation of equilibrium, thermodynamic and kinetic parameters," *Bioresource Technology*, vol. 99, no. 8, pp. 3057–3065, 2008.

[6] M. J. Pollock, "Neutralizing dyehouse wastes with flue gases and decolorizing with fly ash," *The American Dyestuff Reporter*, vol. 62, no. 8, pp. 21–23, 1973.

[7] M. K. Purkait, A. Maiti, S. DasGupta, and S. De, "Removal of congo red using activated carbon and its regeneration," *Journal of Hazardous Materials*, vol. 145, no. 1-2, pp. 287–295, 2007.

[8] M. G. Eilbeck, *Chemical Process in Water Waste Treatment*, John Wiley & Sons, Chichester, UK, 1985.

[9] M. K. Purkait, S. DasGupta, and S. De, "Micellar enhanced ultrafiltration of eosin dye using hexadecyl pyridinium chloride," *Journal of Hazardous Materials*, vol. 136, no. 3, pp. 972–977, 2006.

[10] M. K. Purkait, S. DasGupta, and S. De, "Removal of dye from waste water using micellar enhanced ultra fitrationn and recovery of surfactant," *Journal of Separation and Purification Technology*, vol. 37, pp. 81–92, 2003.

[11] S. Chakraborty, M. K. Purkait, S. DasGupta, S. De, and J. K. Basu, "Nanofiltration of textile plant effluent for color removal and reduction in COD," *Separation and Purification Technology*, vol. 31, no. 2, pp. 141–151, 2003.

[12] M. Mohammadi, A. J. Hassani, A. R. Mohamed, and G. D. Najafpour, "Removal of rhodamine B from aqueous solution using palm shell-based activated carbon: adsorption and kinetic studies," *Journal of Chemical and Engineering Data*, vol. 55, no. 12, pp. 5777–5785, 2010.

[13] G. Crini, "Non-conventional low-cost adsorbents for dye removal: a review," *Bioresource Technology*, vol. 97, no. 9, pp. 1061–1085, 2006.

[14] M. Doğan, Y. Özdemir, and M. Alkan, "Adsorption kinetics and mechanism of cationic methyl violet and methylene blue dyes onto sepiolite," *Dyes and Pigments*, vol. 75, no. 3, pp. 701–713, 2007.

[15] C. Chen, M. Zhang, Q. Guan, and W. Li, "Kinetic and thermodynamic studies on the adsorption of xylenol orange onto MIL-101(Cr)," *Chemical Engineering Journal*, vol. 183, pp. 60–67, 2012.

[16] Z. Ioannou, C. Karasavvidis, A. Dimirkou, and V. Antoniadis, "Adsorption of methylene blue and methyl red dye from aqueous solutions onto modified zeolite," *Journal of Water Science and Technology*, vol. 67, no. 5, pp. 1129–1136, 2013.

[17] N. A. Oladoja, C. O. Aboluwoye, and A. O. Akinkugbe, "Evaluation of loofah as a sorbent in the decolorization of basic dye contaminated aqueous system," *Industrial and Engineering Chemistry Research*, vol. 48, no. 6, pp. 2786–2794, 2009.

[18] J. C. Liu, S. Ma, and L. J. Zang, "Preparation and characterization of ammonium-functionalized silica nano particle as new adsorbent to remove methyl orange from aqueous solution," *Journal of Applied Surface Science*, vol. 265, pp. 393–398, 2013.

[19] B. K. Nandi, A. Goswami, and M. K. Purkait, "Adsorption characteristics of brilliant green dye on kaolin," *Journal of Hazardous Materials*, vol. 161, no. 1, pp. 387–395, 2009.

[20] I. D. Mall, V. C. Srivastava, and N. K. Agarwal, "Removal of Orange-G and Methyl Violet dyes by adsorption onto bagasse fly ash—kinetic study and equilibrium isotherm analyses," *Dyes and Pigments*, vol. 69, no. 3, pp. 210–223, 2006.

[21] R. Gong, Y. Ding, M. Li, C. Yang, H. Liu, and Y. Sun, "Utilization of powdered peanut hull as biosorbent for removal of anionic dyes from aqueous solution," *Dyes and Pigments*, vol. 64, no. 3, pp. 187–192, 2005.

[22] A. Z. Aroguz, J. Gulen, and R. H. Evers, "Adsorption of methylene blue from aqueous solution on pyrolyzed petrified sediment," *Bioresource Technology*, vol. 99, no. 6, pp. 1503–1508, 2008.

[23] N. A. Oladoja and A. K. Akinlabi, "Congo red biosorption on palm kernel seed coat," *Industrial and Engineering Chemistry Research*, vol. 48, no. 13, pp. 6188–6196, 2009.

[24] S. Dawood and T. K. Sen, "Removal of anionic dye Congo red from aqueous solution by raw pine and acid-treated pine cone powder as adsorbent: equilibrium, thermodynamic, kinetics, mechanism and process design," *Water Research*, vol. 46, no. 6, pp. 1933–1946, 2012.

[25] R. L. M. Allen, *Colour Chemistry*, Appleton-Century Crofts Education Division, 1971.

[26] A. Mittal, D. Kaur, and J. Mittal, "Applicability of waste materials—bottom ash and deoiled soya—as adsorbents for the removal and recovery of a hazardous dye, brilliant green," *Journal of Colloid and Interface Science*, vol. 326, no. 1, pp. 8–17, 2008.

[27] Y. Kismir and A. Z. Aroguz, "Adsorption characteristics of the hazardous dye brilliant green on Saklıkent mud," *Chemical Engineering Journal*, vol. 172, no. 1, pp. 199–206, 2011.

[28] H. W. Yeung, W. W. Li, and T. B. Ng, "Isolation of a ribosome-inactivating and abortifacient protein from seeds of Luffa acutangula," *International Journal of Peptide and Protein Research*, vol. 38, no. 1, pp. 15–19, 1991.

[29] H. Demir, A. Top, D. Balköse, and S. Ülkü, "Dye adsorption behavior of *Luffa cylindrica* fibers," *Journal of Hazardous Materials*, vol. 153, no. 1-2, pp. 389–394, 2008.

[30] O. Abdelwahab, "Evaluation of the use of loofa activated carbons as potential adsorbents for aqueous solutions containing dye," *Desalination*, vol. 222, no. 1–3, pp. 357–367, 2008.

[31] K. G. Bhattacharyya and A. Sarma, "Adsorption characteristics of the dye, brilliant green, on neem leaf powder," *Dyes and Pigments*, vol. 57, no. 3, pp. 211–222, 2003.

[32] V. S. Mane, I. D. Mall, and V. C. Srivastava, "Kinetic and equilibrium isotherm studies for the adsorptive removal of brilliant green dye from aqueous solution by rice husk ash," *Journal of Environmental Management*, vol. 84, no. 4, pp. 390–400, 2007.

[33] L. S. Balistrieri and J. W. Murray, "The surface chemistry of goethite (alpha-FeOOH) in major ion seawater," *The American Journal of Science*, vol. 281, no. 6, pp. 788–806, 1981.

[34] A. I. Vogel, *Text Book of Practical Organic Chemistry*, Longman, London, UK, 1970.

[35] V. O. A. Tanobe, T. H. D. Sydenstricker, M. Munaro, and S. C. Amico, "A comprehensive characterization of chemically treated Brazilian sponge-gourds (*Luffa cylindrica*)," *Polymer Testing*, vol. 24, no. 4, pp. 474–482, 2005.

[36] M. A. H. Hassan, L. M. A. Fayoumi, and M. M. Jamal, "Kinetic study of the discoloration of triphenylmethane dyes as a function of pH, salt effect," *Journal of the University of Chemical Technology and Metallurgy*, vol. 46, pp. 395–400, 2011.

[37] J. D. Roberts and M. C. Caserio, *Basic Principle of Organic Chemistry*, W. A. Benjamin, Inc., Menlo Park, Calif, USA, 2nd edition, 1977.

[38] O. K. Júnior, L. V. A. Gurgel, R. P. de Freitas, and L. F. Gil, "Adsorption of Cu(II), Cd(II), and Pb(II) from aqueous single metal solutions by mercerized cellulose and mercerized sugarcane bagasse chemically modified with EDTA dianhydride (EDTAD)," *Carbohydrate Polymers*, vol. 77, no. 3, pp. 643–650, 2009.

[39] A. C. A. da Costa, L. M. S. de Mesquita, and J. Tornovsky, "Batch and continuous heavy metals biosorption by a brown seaweed from a zinc-producing plant," *Minerals Engineering*, vol. 9, no. 8, pp. 811–824, 1996.

[40] Q. Sun and L. Yang, "The adsorption of basic dyes from aqueous solution on modified peat-resin particle," *Water Research*, vol. 37, no. 7, pp. 1535–1544, 2003.

[41] S. Lanregren, "About the theory of so-called adsorption of soluble substances," *Kungliga Svenska Vetenskapsakademiens Handlingar*, vol. 24, no. 4, pp. 1–39, 1889.

[42] Y. S. Ho, "Review of second-order models for adsorption systems," *Journal of Hazardous Materials*, vol. 136, no. 3, pp. 681–689, 2006.

[43] L. Zeng, X. M. Li, and J. D. Liu, "Adsorptive removal of phosphate from aqueous solutions using iron oxide tailings," *Water Research*, vol. 38, no. 5, pp. 1318–1326, 2004.

[44] J. Zeldowitsch, "Über den mechanismus der katalytischen oxydation von CO an MnO_2," *Acta Physicochimica URSS*, vol. 1, pp. 449–464, 1934.

[45] Y. S. Ho and G. McKay, "Sorption of dye from aqueous solution by peat," *Chemical Engineering Journal*, vol. 70, no. 2, pp. 115–124, 1998.

[46] Y. S. Ho and A. E. Ofomaja, "Pseudo-second-order model for lead ion sorption from aqueous solutions onto palm kernel fiber," *Journal of Hazardous Materials*, vol. 129, no. 1–3, pp. 137–142, 2006.

[47] Y. S. Ho and G. McKay, "A kinetic study of dye sorption by biosorbent waste product pith," *Resources, Conservation and Recycling*, vol. 25, no. 3-4, pp. 171–193, 1999.

[48] W. J. Weber and J. C. Morris, "Kinetics of adsorption on carbon from solution," *Journal of Sanitary Engineering Division*, vol. 89, pp. 31–59, 1963.

[49] N. Kannan and M. M. Sundaram, "Kinetics and mechanism of removal of methylene blue by adsorption on various carbons—a comparative study," *Dyes and Pigments*, vol. 51, no. 1, pp. 25–40, 2001.

[50] K. K. Panday, G. Prasad, and V. N. Singh, "Copper(II) removal from aqueous solutions by fly ash," *Water Research*, vol. 19, no. 7, pp. 869–873, 1985.

[51] U. R. Lakshmi, V. C. Srivastava, I. D. Mall, and D. H. Lataye, "Rice husk ash as an effective adsorbent: evaluation of adsorptive characteristics for indigo carmine dye," *Journal of Environmental Management*, vol. 90, no. 2, pp. 710–720, 2009.

[52] V. S. Mane and P. V. V. Babu, "Studies on the adsorption of brilliant green dye from aqueous solution onto low-cost NaOH treated saw dust," *Desalination*, vol. 273, no. 2-3, pp. 321–329, 2011.

[53] G. E. Boyd, A. W. Adamson, and L. S. Myers Jr., "The exchange adsorption of ions from aqueous solutions by organic zeolites. II. Kinetics," *Journal of the American Chemical Society*, vol. 69, no. 11, pp. 2836–2848, 1947.

[54] Y. S. Ho, T. H. Chiang, and Y. M. Hsueh, "Removal of basic dye from aqueous solution using tree fern as a biosorbent," *Process Biochemistry*, vol. 40, no. 1, pp. 119–124, 2005.

[55] K. R. Hall, L. C. Eagleton, A. Acrivos, and T. Vermeulen, "Pore- and solid-diffusion kinetics in fixed-bed adsorption under constant-pattern conditions," *Industrial and Engineering Chemistry Fundamentals*, vol. 5, no. 2, pp. 212–223, 1966.

[56] H. M. F. Freundlich, "Ube die adsorption in losurgen," *Zeitschrift für Physikalische Chemie A*, vol. 57, pp. 385–470, 1906.

[57] V. S. Mane, I. D. Mall, and V. C. Srivastava, "Use of bagasse fly ash as an adsorbent for the removal of brilliant green dye from aqueous solution," *Dyes and Pigments*, vol. 73, no. 3, pp. 269–278, 2007.

[58] I. A. W. Tan, B. H. Hameed, and A. L. Ahmad, "Equilibrium and kinetic studies on basic dye adsorption by oil palm fibre activated carbon," *Chemical Engineering Journal*, vol. 127, no. 1–3, pp. 111–119, 2007.

[59] G. A. Holdgate and W. H. J. Ward, "Measurements of binding thermodynamics in drug discovery," *Drug Discovery Today*, vol. 10, no. 22, pp. 1543–1550, 2005.

[60] P. V. Messina and P. C. Schulz, "Adsorption of reactive dyes on titania-silica mesoporous materials," *Journal of Colloid and Interface Science*, vol. 299, no. 1, pp. 305–320, 2006.